Akademie věd České republiky

Teze disertace
k získání vědeckého titulu "doktor věd"
ve skupině věd *Technické vědy*

# *Micromechanical modeling of heterogeneous materials and structures*

název disertace

Komise pro obhajoby doktorských disertací v oboru
*Mechanika těles, konstrukcí, mechanismu a prostředí*

Jméno uchazeče: Michal Šejnoha

Pracoviště uchazeče: ČVUT Fakulta stavební, Katedra mechaniky

Místo a datum: v Praze 20. 12. 2007

# Resumé

Teze disertace jsou souhrnem výpočetních postupů a výsledků numerických simulací prezentovaných v rámci příspěvků obsažených v prvních třech kapitolách disertace. Pozornost je zaměřena na víceúrovňové modelování kompozitů uhlík-uhlík (C/C) s plátnovou vazbou.

Vlivem použitých výrobních procesů vykazují tyto materiálové systémy určitý stupeň geometrické neuspořádanosti charakterizované řadou imperfekcí, a to nejen na úrovni jednotlivých svazků vláken či plátnové vazby, ale i na makroúrovni, tedy na úrovni určité vícevrstvé konstrukce. Ukazuje se, že tyto imperfekce mají zásadní význam pro predikci výsledných efektivních materiálových vlastností na všech úrovních. Stěžejním krokem analýzy textilních kompozitů tedy zůstává spolehlivá kvantifikace jednotlivých systémů imperfekcí.

Zatímco na mikroúrovni hovoříme víceméně o náhodném úspořádání vláken v příčném řezu jednotlivých svazků, tak na mezoúrovni a makroúrovni se již jedná o určité poruchy vnitřní struktury plátnové vazby s nepravidelným uspořádáním jednotlivých vrstev v celém laminátu. Příkladem jsou vzájemné posuny vrstev, nerovnoměrná výška jednotlivých svazků vláken či nepravidelné zvlnění v jejich podélném směru. Nejdůležitější skupinu poruch však představuje vnitřní pórovitost C/C kompozitů, která v některých případech dosahuje až 30% celkového objemového zastoupení. Významnou roli při kvantifikaci jednotlivých typů geometrických imperfekcí a poruch vnitřní struktury materiálů hraje v tomto případě obrazová analýza.

V práci byl použit systém analýzy obrazu LUCIA G, umožňující převedení původně barevného obrazu na obraz binární. Binárních obrazů skutečné mikrostruktury lze pak přímo využít při popisu této mikrostruktury pomocí různých statistických deskriptorů, jakými jsou například jednobodová a dvoubodová pravděpodobnostní funkce a “Lineal path” funkce. Informace obsažené v jednobodové a dvoubodové pravděpodobnostní funkci lze přímo využít při analýze skutečných materiálových systémů, a to ve spojení s rozšířenými Hashin-Shtrikmanovými

variačními principy. Takováto analýza se však většinou omezuje pouze na mikroúroveň. Na mezoúrovni anebo v případě, kdy je třeba postihnout detailní průběh lokálních polí napětí a deformace, vyžaduje analýza aplikaci reprezentativního objemového modelu v podobě periodické jednotkové buňky ve spojení s homogenizací prvního řádu. V případě nepravidelných struktur pak hovoříme o tak zvané statisticky ekvivalentní periodické buňce (SEPUC) odvozené na základě formulace vhodného optimalizačního problému. V našem případě se ověděil postup založený na minimalizaci čverců rozdílů dvoubodové funkce pravděpodobnosti skutečné mikrostruktury a mikrostruktury aproximované jednotkovou buňkou.

Vedle již zmíněných výpočtů založených na aplikaci Hashin-Shtrikmanových variačních postupů nacházejí své uplatnění i další klasické mikromechanické modely, a to nejen na mikroúrovni, ale i na mesoúrovni, kdy informace o mikrostruktuře jsou omezeny například na histogramy rozložení úhlu orientace svazků vláken v jejich podélném směru. Metoda Mori-Tanaka v tomto případě nabízí vhodnou alternativu v porovnání s výpočetně podstatně náročnějšími numerickými simulacemi na bázi metody konečných prvků.

Zvláštní kategorii poruch struktury materiálu představuje pórovitost. Nevyhnutelnost zavedení porozity při predikci efektivních vlastností C/C kompozitů byla zatím ověřena v rámci studie dvourozměrného vedení tepla. Rozšíření této problematiky na stanovení makroskopických deformačních charakteristik, ať už v rámci periodické homogenizace, nebo užitím mikromechanických metod, je předmětem současného výzkumu.

Podrobnější popis jednotlivých bodů obsažených v předchozích odstavcích je náplní kapitol 3 až 5. Kapitola 3 je věnována popisu mikrostruktury na úrovni plátnové vazby. Výsledky jsou následně použity v kapitole 4, a to jednak při formulaci vhodné statisticky ekvivalentní periodické buňky a jednak v přímém spojení s klasickou mikromechanickou metodou Mori-Tanaka. Předložené homogenizační postupy však postrádají jakékoliv informace o pórovitosti. Tomuto zásadnímu nedostatku, který je nyní předemětem intenzivního výzkumu, je věnována kapitola 5. Závěrečná kapitola pak podává souhrn dosažených výsledků a naznačuje určité směry dalšího výzkumu v oblasti C/C kompozitů.

# Obsah

# Micromechanical modeling of plain weave imperfect C/C composites

## 1 Summary

After fabrication the carbon-carbon (C/C) plain weave textile composites often show a certain degree of geometrical or material disorder including yarn waviness and misalignment or nesting of individual fiber tows together with intrinsic material porosity observed at all relevant scales. A brief survey of recently developed approaches for estimating overall elastic stiffnesses or thermal conductivities of such composite systems is presented in this paper. Depending on the source and type of available geometrical data the homogenization scheme usually relies either on finite element (FEM) simulations performed for a suitable Periodic Unit Cell (PUC) or employs one of the popular averaging techniques such as the Mori-Tanaka (MT) method. While existing applications of both methodologies are encouraging, there still exists a number of steps to be completed in the course of the future research.

# 2 INTRODUCTION

Fiber-reinforced composites present a well-established and attractive material variant used in numerous branches of engineering design with applications ranging from rehabilitation and repair of concrete and masonry structures to design of bio-compatible medical implants [37]. In comparison with traditional materials, composites offer higher strength, light weight, non-corrosive properties, dimensional stability, good conformability and possibility of performance-based design. Among the most prominent material systems exhibiting these properties remain plain weave textile composites produced by orthogonal interlacing of yarns bonded to either polymeric or pyrolytic carbon matrix. An ever growing interest in these material systems is further promoted by their appealing mechanical performance, superior impact tolerance and wear resistance [7].

Although frequently used in practice, an accurate and reliable mechanical analysis of woven composites still presents a considerable challenge owing to their complex geometry displayed at several length scales. In this paper the C/C plain weave textile composite is adopted as one particular representative of these complex geometries. Apart from nontrivial geometrical texture of textile composites in general, the C/C composites in particular, see Fig. 1, are prone to various types of geometrical imperfections and relatively high porosity arising directly from the process of fabrication, which is characterized by thermal decomposition and transformation of an initial polymeric precursor into the pyrolytic carbon matrix through several steps of carbonization, re-impregnation and final graphitization [5, 36]. As further evident from Fig. 1, the major contribution to the porosity, which may exceed 30% of the overall volume [44, 46], is due to crimp voids and delamination cracks, which are usually classified as inter-tow voids (Fig. 1(a)), as well as due to intra-tow voids represented by pores and transverse cracks (Fig. 1(b)), see [45] for more details.

A reliable and accurate description of such material systems thus requires the following major aspects to be taken into account:

- Geometrical imperfections represented by yarn waviness, its cross-sectional variability together with their misalignment and nesting

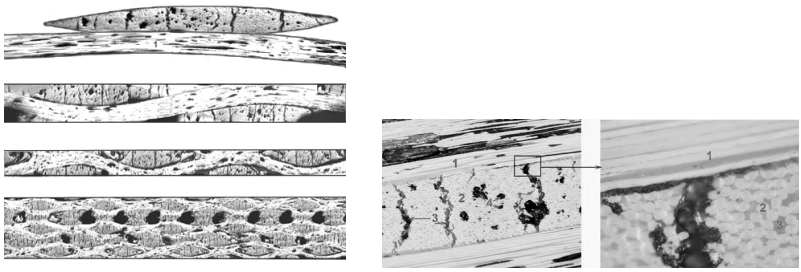

(a) (b)

Fig. 1: Color images of a real composite system: (a) Scheme of multiscale structural model (from top - transverse and longitudinal view of fiber tow composite, composite unit cell, composite lamina, composite plate), (b) Carbon tow microstructure showing major pores and transverse cracks.

within the laminate structure, see Fig. 1($a_4$).

- High porosity of C/C composites on both the microscale (level of individual yarns, Fig. 1(b)) and mesoscale (level of individual plies, Fig. 1($a_2$)).

The purpose of this paper is to provide an overview of recently developed approaches that allow, at least to some extent, for incorporating the above items into the predictions of the mechanical and thermal properties of C/C composites. Application of classical micromechanical schemes such as the Mori-Tanaka method as well as detailed finite element simulations that assume an existence of a certain representative periodic unit cell will be discussed. Since the present survey is still a part of an ongoing research the two approaches will be presented with all their current limitations. Nevertheless, possible routes for their improvement will be given.

The rest of the paper is organized as follows:

- Quantification of the real meso structure through a laborious eva-

luation of images of real material samples is briefly addressed in Section 3. The format of available information then drives the selection of a particular numerical model.

- Neglecting the material porosity, a hardly justified step for C/C composites but acceptable for carbon-polymer (C/P) composites, we proceed in Section 4 with the modeling of dominant geometrical imperfections previously quantified. An idealized three-dimensional periodic unit cell originally formulated in [25] is briefly outlined in Section 4.1 together with essential steps of the FEM based simulations in the framework of the first-order homogenization techniques. This unit cell then serves as a point of departure for the formulation of the Mori-Tanaka method presented in Section 4.2 as well as more complex finite element simulations discussed in Section 4.3 particularly in conjunction with the construction of so called Statistically Equivalent Periodic Unit Cell (SEPUC).

- Section 5 then offers possible routes for incorporating the material porosity into computational modeling. A simple example of multiscale two-dimensional finite element simulation of heat conduction problem with emphases on material porosity is presented.

- Several concluding remarks suggesting the main stream of the current research are given in Section 6.

# 3 Microstructure evaluation

Elastic as well as inelastic behavior of textile composites assuming well defined geometry has been examined in many theoretical studies [53, 7, 6, 10, 11, 9]. Comparable investigations addressing the behavior of actual material systems have emerged, however, only recently [54, 27, 58]. It has been reported that actual microstructure, not reflected in idealized computational models, may have a significant impact on model predictions. A sufficiently detailed quantitative analysis of the real microstructure is therefore desirable. In this section we describe the essential results of such an analysis when applied to plain weave textile composites.

Fig. 2(a) shows a particular composite laminate consisting of eight layers of carbon fabric Hexcel G 1169 bonded to a carbon matrix. The total of twenty such specimens having dimensions of $25 \times 2.5 \times 2.5$ mm were fixed into the epoxy resin and after curing subjected to final surface grounding and polishing using standard metallographic techniques to produce specimens suitable for the subsequent image analysis.

Using the results provided by image analysis software **LUCIA G** allows us to derive the frequency spectrum of the Fourier series which in turn can be used to describe the variation of the yarn shape along its longitudinal direction [19, 21, 20]. As reported in [22, 51] the crimp waveform is subject to deformation when pressed during the manufacturing process and the frequency spectrum is therefore distorted compared to that of the unprocessed (free) fabric. Deformation of reinforcements such as the nonuniform waviness and to some extent also the mutual shift of individual layers also visible in Fig. 2(a) can be reflected through histograms of inclination angles derived from centerlines of individual yarns, see Figs. 2(e)(f) and [51] for more details. We describe in Section 4.2 how these micrographs can be effectively used to provide efficient estimates of the overall elastic response of the composite employing the Mori-Tanaka micromechanical model.

Nonuniform waviness of the yarn, however, is not the only imperfection observed in real material systems. Nonuniform cross-sectional aspect ratio of yarns, their misalignment in the textile plane and nesting have been already mentioned. All these imperfections can be clearly iden-

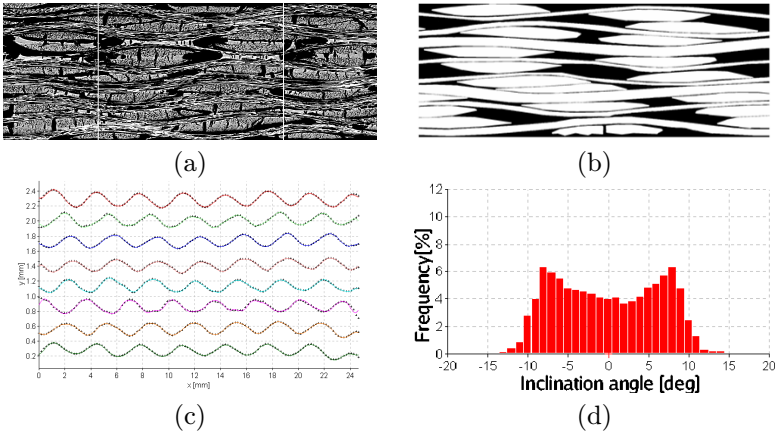


Fig. 2: Quantification of microstructure: a) color image of real composite sample, b) binary image, c) approximation of centerlines, d) distribution of inclination angles

tified from binary images of actual microstructures such as the one plotted in Fig. 2(b). Several such sections taken from various locations of the laminate are usually examined to provide for averages of various geometrical parameters including dimensions, shape of the yarn cross-section and its thickness, etc. The resulting statistics are stored in Table 1.

Tab. 1: Quantification of microstructure [44, 46]

| statistics [$\mu m$] | a | h | b | g |
|---|---|---|---|---|
| Average | 2250 | 300 | 150 | 400 |
| Standard deviation | 155 | 50 | 20 | 105 |

We emphasize that neglecting the porous phase, as has been done when generating the respective binary images, may cause severe overestimation of the expected overall properties. When, on the other hand,

comparisons of various computational strategies (averaging schemes and PUC analyses) are of the main interest, we may accept such limitation and use the values from Table 1 to construct an ideal periodic unit cell based on the geometrical model proposed in [25]. Geometrical details of the unit cell are plotted in Fig. 3. This particular approach is adopted in Section 4.2 to provide for reference values of the effective stiffness when searching for a suitable geometrical representation of a yarn for which the closed form solution of the Eshelby tensor is available. Another application is discussed in Section 5.1 with reference to effective thermal conductivities.

Detailed evaluation of individual images is on the other hand a relatively tedious task. To avoid this step, we introduced in our previous works [57, 58, 59] the concept of statistically equivalent periodic unit cell derived by matching the material statistics of real and simplified microstructures. It is of interest to point out, see also [58], that application of this strategy in conjunction with a simple computational model of Fig. 3 failed to represent most of the assumed imperfections. To remedy this situation, the authors proposed an extension of the original model given in terms of a two-layered PUC displayed in Fig. 6. The essential modeling steps are outlined in Section 4.3. Further details can be found in [60].

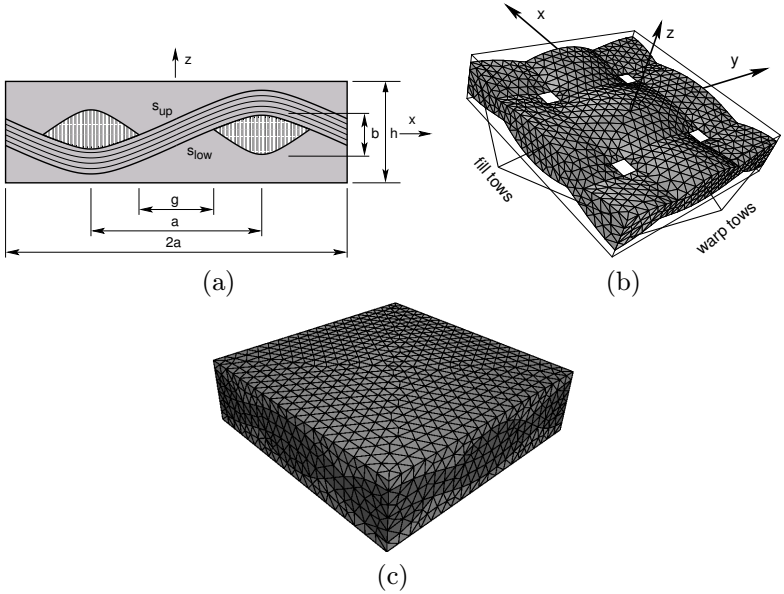


Fig. 3: Idealized periodic unit cell: a) cross-section of an equivalent periodic unit cell, b) three-dimensional view, c) finite element mesh

# 4 Treating geometrical imperfections

In this section two computational strategies are considered to treat actual or imperfect composites depending on the available input data discussed in the previous section. Since both approaches rely on the finite element analysis of a periodic unit cell, we begin in Section 4.1 with a brief summary of the application of the first order homogenization in the framework presented in [31].

## 4.1 Idealized periodic unit cell

Consider a representative volume element given, e.g. in terms of the PUC in Fig. 3(b). To obtain the resulting discretized model shown in Fig. 3(c) the principles of matched mesh generation [52, 29] were implemented into Advancing Front method-based automated mesh generator **T3D** [40]. Identical approach can be adopted for more complex geometries such as the one proposed in Section 4.3.

The theoretical formulation now proceeds as follows. Suppose that the periodic unit cell in Fig. 3(c) is loaded by kinematically admissible macroscopic uniform strain $\boldsymbol{E}$. In view of the assumed microstructure periodicity the local displacement field $\mathbf{u}(\mathbf{x})$ then admits the following decomposition

$$\mathbf{u}(\mathbf{x}) = \boldsymbol{E} \cdot \mathbf{x} + \mathbf{u}^*(\mathbf{x}), \tag{1}$$

where $\mathbf{u}^*(\mathbf{x})$ represents a periodic fluctuation of $\mathbf{u}(\mathbf{x})$ due to the presence of heterogeneities. The local strain tensor then assumes the form

$$\boldsymbol{\varepsilon}(\mathbf{x}) = \boldsymbol{E} + \boldsymbol{\varepsilon}^*(\mathbf{x}), \tag{2}$$

where the fluctuating part $\boldsymbol{\varepsilon}^*(\mathbf{x})$ vanishes upon the volume averaging. Next, introducing Eq. (2) into the principle of virtual work (the Hill-Mandel lemma) yields ($\delta\boldsymbol{E} = 0$ for prescribed $\boldsymbol{E}$)

$$\delta\boldsymbol{E} : \boldsymbol{\Sigma} = 0 = \langle \delta\boldsymbol{\varepsilon}(\mathbf{x}) : \boldsymbol{\sigma}(\mathbf{x}) \rangle = \left\langle \delta\boldsymbol{\varepsilon}^{\ell}(\mathbf{x}) : \boldsymbol{\sigma}^{\ell}(\mathbf{x}) \right\rangle = \left\langle \delta\boldsymbol{\varepsilon}^{*\ell}(\mathbf{x}) : \boldsymbol{\sigma}^{\ell}(\mathbf{x}) \right\rangle, \tag{3}$$

where $\langle\cdot\rangle$ stands for the volumetric averaging with respect to the PUC and $\cdot^{\ell}$ is used to denote a quantity in the local coordinate system. The local stress field then reads

$$\boldsymbol{\sigma}^{\ell}(\mathbf{x}) = \mathbf{L}^{\ell}(\mathbf{x}) : \left(\boldsymbol{E}^{\ell} + \boldsymbol{\varepsilon}^{*\ell}(\mathbf{x})\right), \tag{4}$$

where $\mathbf{L}^{\ell}$ is the material stiffness tensor. Relating the strain tensors in the local and global coordinate systems by well-known relations $\boldsymbol{E}^{\ell} = \mathbf{T}_{\varepsilon} : \boldsymbol{E}$, $\boldsymbol{\varepsilon}^{*\ell} = \mathbf{T}_{\varepsilon} : \boldsymbol{\varepsilon}^{*}$, see e.g. [4], and inserting Eq. (4) into Eq. (3) yields the stationarity condition of a given problem in the form

$$0 = \left\langle \delta\boldsymbol{\varepsilon}^{*}(\mathbf{x}) : \mathbf{T}_{\varepsilon}(\mathbf{x}) : \left[\mathbf{L}^{\ell}(\mathbf{x}) : \mathbf{T}_{\varepsilon}(\mathbf{x}) : (\boldsymbol{E} + \boldsymbol{\varepsilon}^{*}(\mathbf{x}))\right] \right\rangle, \tag{5}$$

to be satisfied for all kinematically admissible variations $\delta\boldsymbol{E}$ and $\delta\boldsymbol{\varepsilon}^{*}$.

The volume averages of the local stresses derived from the solutions of six independent elasticity problems, in which one of the components of the macroscopic strain vector $\boldsymbol{E}$ is set equal to one while the others vanish, then furnish individual columns of the $6 \times 6$ macroscopic homogenized stiffness matrix $\mathbf{L}^{\mathrm{FEM}}$.

## 4.2 Application of the Mori-Tanaka method

The lack of periodicity, presence of imperfections or random nature of actual microstructures often favored the use of well established effective media (effective field) theories [48, 17]. If reflecting the essential details of the underlying microstructure they yield acceptable accuracy over a wide range of material systems. Among others the Mori-Tanaka method has earned a considerable interest particularly due to its explicit nature [32, 1]. Although this method has been extensively used to provide estimates of overall composite response in many engineering applications its use in the field of textile composites emerged only recently with reference to knitted composites [14].

In the case of imperfect plain weave textile composites the following main objectives can be stated: (a) to introduce the non-uniformities of the yarn path represented by histograms of inclination angle distribution into the micromechanical model; (b) to identify an appropriate shape of

an equivalent inclusion substituting actual yarns; (c) to assess its optimal dimensional description, which establishes certain links to geometrical uncertainties of real systems other than those contained in histograms of Fig. 2(d).

To begin we summarize the essence of this method in the form presented in [14]. In particular, consider an $N$-phase composite with a distinguishable matrix phase having the stiffness tensor $\mathbf{L}_0$ and being reinforced by $N-1$ families of ellipsoidal heterogeneities. Each heterogeneity is characterized by the stiffness tensor $\mathbf{L}_r$ and occupies a volume $\Omega_r$. With reference to [1] the Mori-Tanaka estimates of the overall stiffness tensor $\mathbf{L}$ reads

$$\mathbf{L}^{\mathrm{MT}} = \mathbf{L}_0 + \left( \sum_{r=1}^{N-1} c_r \left( \mathbf{L}_r - \mathbf{L}_0 \right) \mathbf{T}_r \right) \left( c_0 \mathbf{I} + \sum_{r=1}^{N-1} c_r \mathbf{T}_r \right)^{-1}, \tag{6}$$

where $c_r$ denotes the volume fraction of the $r$-th phase. The corresponding partial stress concentration factor $\mathbf{T}_r$ has the form

$$\mathbf{T}_r = \left( \mathbf{I} + \mathbf{P}_r \left( \mathbf{L}_r - \mathbf{L}_0 \right) \right)^{-1}, \tag{7}$$

where the $\mathbf{P}_r$ tensor is provided by

$$\mathbf{P}_r = \int_{\Omega_r} \mathbf{\Gamma}_0(\mathbf{x} - \mathbf{x}') \, \mathrm{d}\mathbf{x}'. \tag{8}$$

Function $\mathbf{\Gamma}_0$ is related to Green's function of an infinite medium with stiffness tensor $\mathbf{L}_0$. It follows from the classical Eshelby work [8] that $\mathbf{P}_r$ for ellipsoidal inclusions is constant and can be evaluated as

$$\mathbf{P}_r = \mathbf{S}_r \mathbf{L}_0^{-1}, \tag{9}$$

where $\mathbf{S}_r$ is the Eshelby tensor. When the matrix phase is isotropic, explicit expressions for $\mathbf{S}_r$ can be found in [8].

As pointed out in [2, 3] the Mori-Tanaka method provides diagonally symmetric estimates of the overall stiffness matrix in two-phase systems of any phase geometry, and in multiple systems which are reinforced by aligned inclusions of identical shape. To arrive at diagonally symmetric

predictions for the studied system we proceed as follows. First, consider a two-phase material system ($N = 2$) consisting of an isotropic matrix reinforced by identical heterogeneities with different orientations. Suppose for a moment that all heterogeneities posses the same orientation. Then, the overall stiffness tensor is symmetric [2] and can be decomposed as

$$\mathbf{L}^{\mathrm{MT}} = \mathbf{L}_0 + c_1 \left( (\mathbf{L}_1 - \mathbf{L}_0) \, \mathbf{T}_1 \right) \left( (1 - c_1)\mathbf{I} + c_1 \mathbf{T}_1 \right)^{-1} = \mathbf{L}^{(0)} + c_1 \mathbf{L}^{(1)}. \quad (10)$$

Notice that due to assumed isotropy, the tensor $\mathbf{L}^{(0)}$ is independent of the reference coordinate system while $\mathbf{L}^{(1)}$ stores the orientation-dependent part. Following [41], the overall stiffness of the system is defined as

$$\mathbf{L}^{\mathrm{S-TP}} = \{\mathbf{L}^{\mathrm{MT}}\} = \mathbf{L}^{(0)} + c_1 \{\mathbf{L}^{(1)}\}, \quad (11)$$

where the curly brackets $\{\}$ denote averaging over all possible orientations. In particular, when the orientation of each heterogeneity is described using the Euler angles, see Fig. 4, the orientation-dependent part can be

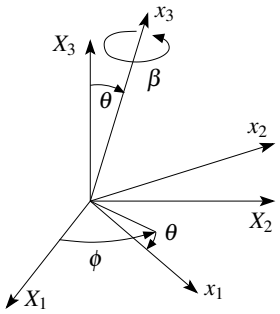


Fig. 4: Definition of the Euler angles

expressed as

$$L^{(1)}_{ijkl}(\theta, \phi, \beta) = a_{ip}(\theta, \phi, \beta) a_{jq}(\theta, \phi, \beta) a_{kr}(\theta, \phi, \beta) a_{ls}(\theta, \phi, \beta) L^{(1)}_{pqrs}(0, 0, 0),$$

where functions $a_{ij}(\theta, \phi, \beta)$ can be found, e.g. in [41, 56, Appendix A].

The orientation average then follows from

$$\{\mathbf{L}^{(1)}\} = \int_0^{2\pi}\int_0^{2\pi}\int_0^{\pi} \mathbf{L}^{(1)}(\theta,\phi,\beta)g(\theta,\phi,\beta)\,\mathrm{d}\theta\,\mathrm{d}\phi\,\mathrm{d}\beta, \qquad (12)$$

where $g(\theta,\phi,\beta)$ denotes the joint probability density describing the distribution of individual angles, here represented by already mentioned histograms of inclination angle. For convenience, the same distribution of angles in two perpendicular directions is assumed to account for three-dimensional nature of the problem. Similar approach was adopted in [38] for three-dimensional orientation distribution of pores derived from two-dimensional images of chemical vapor infiltrated (CVI-infiltrated) carbon felt.

As reported in [43] a sufficient number of histograms is needed to properly account for yarn path imperfections both in the longitudinal and through thickness direction. Several particular examples appear in Fig. 5. The resulting effective stiffnesses then follow from statistical evaluation of a given set of solutions provided by Eq. (11).

To identify an appropriate shape of an equivalent inclusion that drives the solution of the Eshelby problem we recall an ideal PUC discussed in Sections 3 and 4.1. In this particular case, the joint probability density function $g(\theta,\phi,\beta)$ describing the distribution of individual Euler angles for the warp system has the form, recall Fig. 3(b),

$$g(\theta,\phi,\beta) = \begin{cases} 1/(2\alpha) & \text{if } \phi = 0, \beta = 0 \text{ and } \pi/2 - \alpha \le \theta \le \pi/2 + \alpha, \\ 0 & \text{otherwise,} \end{cases}$$

where

$$\alpha = \arctan\left(\frac{b\pi}{2a}\right).$$

Comparing results derived from Eq. (11) with those provided by finite element analysis of an ideal or reference PUC promotes an ellipsoid inclusion as the most appropriate representative of the actual yarn geometry as oppose to rather intuitively expected cylindrical one. These comparative studies further suggest that the choice of the Eshelby tensor, which essentially depends on the ratio of its semi-axes, can hardly be made arbitrary.

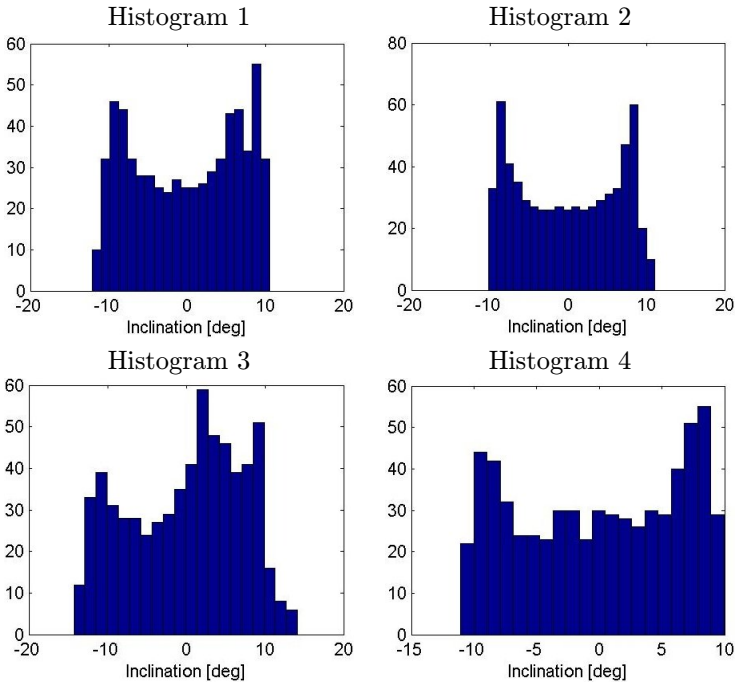


Fig. 5: Real measured histograms of inclination angle [51]

A simple procedure based on the solution of a certain minimization problem is offered in [43] to define an optimal shape of the equivalent ellipsoid. Therein, the optimal values of the ellipsoid semi-axes are found by matching the FEM results with the MT predictions for the reference PUC. To take into account additional uncertainties in the textile geometry a training set of PUCs, rather than a single one, is generated based on the statistical data listed in Table 1. To solve the underlying problem, which consists of the minimization of the error between the FEM and

MT solutions given by

$$E([\mathsf{L}]^{\mathrm{FEM}}, [\mathsf{L}]^{\mathrm{MT}}) = \max_{i=0,\ldots,5, j=0,\ldots,5, \mathsf{B}_{ij}\neq 0} \left| \frac{\mathsf{L}_{ij}^{\mathrm{FEM}} - \mathsf{L}_{ij}^{\mathrm{MT}}}{\mathsf{L}_{ij}^{\mathrm{MT}}} \right|,$$

we employed a version of the genetic algorithm (GA) **GRADE** [15]. Further details can be found in [26, 43]. This step thus completes the last of the three objectives stated in the second paragraph of this section.

## 4.3 Construction of statistically equivalent periodic unit cell

It is often desirable to derive detailed representation of local fields rather than the volume phase averages only as provided by the Mori-Tanaka predictions. Attention is then usually given to periodic unit cell analyses. To exploit the benefit of periodic fields, while at the same time account for uncertainties associated with real microstructures, we introduced in our recent works [57, 58, 59] the concept of statistically equivalent periodic unit cell. This approach will be now briefly reviewed in the context of plain weave textile composites.

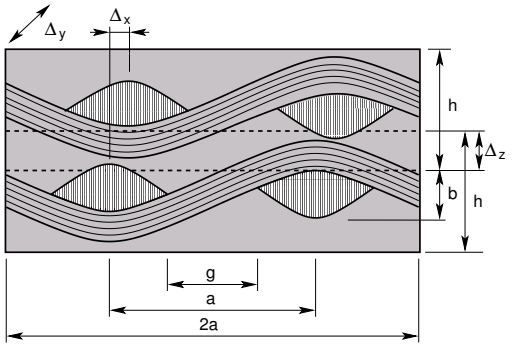


Fig. 6: Scheme of a two-layer idealized unit cell

We expect, see also [58], that reasonably accurate predictions of the overall response of actual multilayered system can be found from the

analysis of a two-layered periodic unit cell shown in Fig. 6. Such a unit cell is fully described by seven independent parameters

$$\mathbf{y} = [a, b, g, h, \Delta_x, \Delta_y, \Delta_z]\,. \tag{13}$$

The principal problem of interest is to determine these parameters such that the resulting macroscopic behavior of the unit cell will compare to that of actual material. The stepping stone of the solution is an ad hoc assumption stating that as long as the two systems are geometrically similar, then they will also yield similar overall response. So far, this has been confirmed for random uniaxial fiber reinforced composites with the fiber volume fraction exceeding 0.4 [57]. Such an assumption then opens the way for quantifying the microstructural details of real and equivalent systems on the bases of various statistical descriptors including the two-point probability function $S(\mathbf{x})$ [49] and the lineal path function $L(\mathbf{x})$ [28]. Both descriptors can be easily computed for digitized microstructures such as the one displayed in Fig. 2(b). In particular, the Fast Fourier transform library **FFTW** [12] is used for the $S$ function, while the sampling template procedure is introduced for the determination of the lineal path function [48].

In our specific case of textile composite it is assumed that the microstructure configuration is characterized by microstructural function associated with (at most) warp and fill directions; i.e. functions $S_w$ and $L_w$ for the warp cross-section and descriptors $S_f$ and $L_f$ for the fill cross-section, recall 3(b). With reference to [55], the following quantities are introduced to measure the similarity between the SEPUC and the original microstructure:

$$F_S^2(\mathbf{y}) = \sum_{p\in\{w,f\}} \sum_{i=i_{min}}^{i_{max}} \sum_{j=j_{min}}^{j_{max}} \left(S_p(\mathbf{y},i,j) - \overline{S_p}\right)^2, \tag{14}$$

$$F_L^2(\mathbf{y}) = \sum_{p\in\{w,f\}} \sum_{i=i_{min}}^{i_{max}} \sum_{j=j_{min}}^{j_{max}} \left(L_p(\mathbf{y},i,j) - \overline{L_p}\right)^2, \tag{15}$$

$$F_{S+L}(\mathbf{y}) = \alpha_S F_S(\mathbf{y}) + \alpha_L F_L(\mathbf{y}), \tag{16}$$

where, e.g. $S_w(\mathbf{y},i,j)$ denotes the two-point probability function deter-

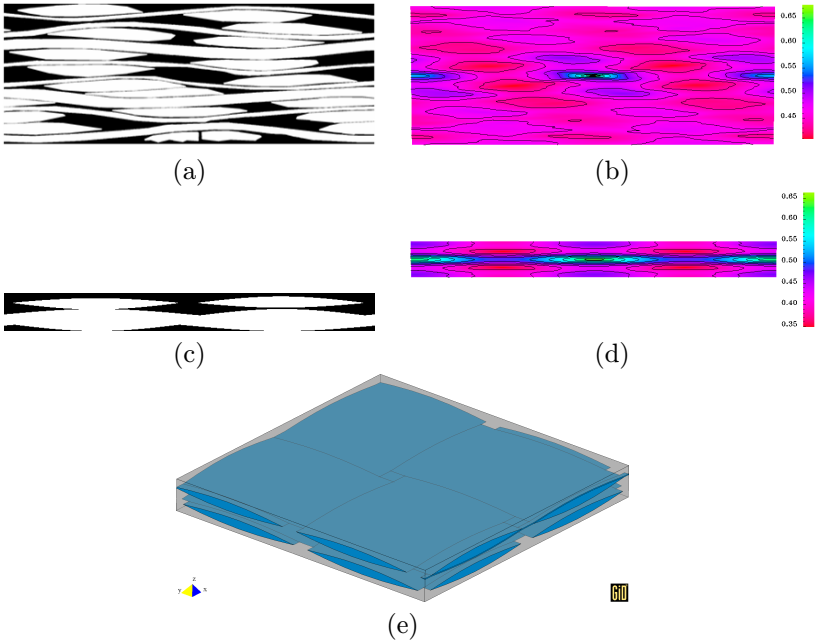


Fig. 7: Target microstructure: a) binary image, b) two-point probability function, Statistically optimal periodic unit cell: c) optimized binary image, d) two-point probability function, e) three-dimensional model

mined for the warp cross-section of a SEPUC described by parameters $\mathbf{y}$ and the value of argument $\mathbf{x} = [i, j]$. The $\alpha_\bullet$ symbol in (16) denotes a scale factor used to normalize the influence of both descriptors.

Finding appropriate dimensions of the unit cell then amounts to the minimization of the above set of equations. The fact that due to the limited bitmap resolution, the objective functions (14)–(16) are discontinuous, promotes again, recall Section 4.2, one of the evolutionary optimization algorithms. Here, the desired solution was delivered with the help of stochastic optimization algorithm **RASA** [30, 16].

Examples of a targeted microstructure and the resulting SEPUC together with the variation of corresponding two-point probability functions $S$ are illustrated in Fig. 7. From the qualitative point of view, it is evident that the statistically optimized unit cell tries to reproduce the matrix rich regions together with the strong nesting of individual layers. Fig. 7 then shows a three-dimensional view of the actual computational model intended for the predictions of the overall mechanical properties in the framework of the first-order homogenization outlined in Section 4.1. The results reported in [60] indicate comparable predictive capabilities of both the Mori-Tanaka method and periodic unit cell simulations for the present material system with limitation to the assumed zero volume of the porous phase. Several routes enabling to overcome this restriction are discussed in Section 6. Primary work on this subject with reference to the solution of heat conduction problem is summarized next.

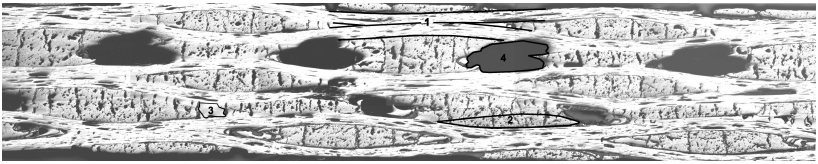

Fig. 8: Representative segment of eight-layer plain weave fabric laminate.

## 5 Treating porosity

Although geometrical imperfections present a distinct source of uncertainties they may prove, in comparison to a very high intrinsic porosity typical of C/C textile composites, far less important particularly from the overall response point of view. This was confirmed in the thesis of Palan [35] who compared theoretical predictions of overall thermal properties of C/C composites assuming an ideal pore-free structure with those obtained experimentally. It was shown that neglecting the porous phase may result in an order of magnitude difference between predicted and measured data. A thirty percent reduction in overall stiffness over the range of 20% of porosity presented in [38] for CVI-infiltrated carbon felts further demonstrates a significant impact of pores on the overall behavior even in the elastic regime. Note that in the case of C/C textile composites the intrinsic porosity may well exceed 30% at the structural level. Despite of that, a little attention has apparently been given to computational models of textile composites that properly account for the presence of pores. The only work we are aware of is due to Kuhn and Charalambides [23, 24]. Unfortunately, a highly idealized geometry of the porous space assumed in their study can hardly accommodate all complexities that appear in real systems.

Fig. 8 shows an actual structure of voids at different scales. The main contribution to the overall porosity due to crimp voids, delamination cracks, matric pores and transverse cracks developed within individual yarns during fabrication can be easily identified. An accurate geomet-

rical quantification of various sources is not a trivial task. Therefore, a relatively simple approach based on the formulation of an ideal periodic unit cell of the type already presented in Section 4.1 is selected as our point of departure. A particular application to evaluation of estimates of overall thermal conductivities is selected on purpose, since the two-dimensional restriction adopted in this study can be well supported by comparative experimental measurements.

## 5.1 Multiscale modeling of heat conduction problem

Suppose that the homogenized effective conductivities of the yarn are already known from an independent micromechanical analysis performed on the level of individual fibers [57, 47]. The objective now is to find these parameters on the mesoscopic level. To that end, we recall the representative section of the composite laminate in Fig. 8. A detailed inspection of this micrograph reveals three more or less periodically repeated geometries. For better view we refer to Figs. 9(a)-(c).

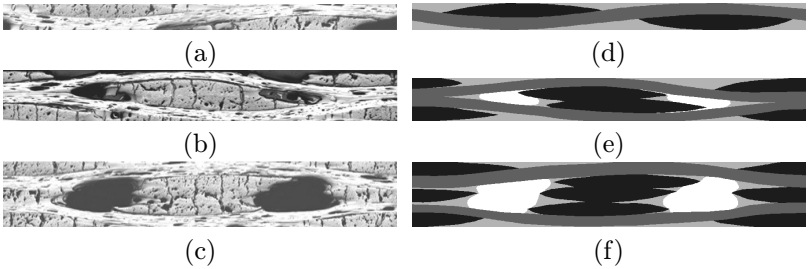


Fig. 9: Homogenization on meso-scale: (a)-(b) PUC1 representing carbon tow-carbon matrix composite, (c)-(d) PUC2 with vacuoles aligned with delamination cracks due to slip of textile plies, (e)-(f) PUC3 with extensive vacuoles representing the parts with textile reinforcement reduction due to bridging effect in the middle ply.

Several such sections taken from various locations of the laminated plates were examined, again with the help of image analyzer **LUCIA G**,

to obtain averages of various parameters including segment dimensions, yarn thickness, shape of the yarn cross-section and also position, size and location of large vacuoles. Approximately 100 measurements were carried out for each segment and subsequently utilized in the formulation of corresponding periodic unit cells displayed in Figs. 9(d)-(f).

Similarities between mechanical and heat conduction problem allows us to continue in the manner analogous to that described in Section 4.1. Hence, the first order homogenization theory is invited again to provide for the effective conductivities. This suggests that the PUC can be loaded along its entire boundary by certain temperature field $\theta(\mathbf{x})$ derived from a uniform mesoscopic temperature gradient $\boldsymbol{H}$. In view of the underlying finite element analysis the local temperature gradient $\boldsymbol{h}(\mathbf{x})$ then admits the following decomposition

$$\boldsymbol{h}(\mathbf{x}) = \boldsymbol{H} + \mathbf{B}(\mathbf{x})\boldsymbol{\theta}_d^*, \tag{17}$$

where $\mathbf{B}(\mathbf{x})$ stores the derivatives of the element shape functions and $\boldsymbol{\theta}_d^*$ lists the nodal values of the fluctuation part of the temperature field being periodic. Assuming steady state conditions the Fourier inequality yields

$$\left\langle \delta\boldsymbol{h}(\mathbf{x})^{\mathsf{T}}\boldsymbol{\chi}(\mathbf{x})\boldsymbol{h}(\mathbf{x})\right\rangle = 0, \tag{18}$$

where $\boldsymbol{\chi}(\mathbf{x})$ is the local (phase) conductivity matrix and $\langle a\rangle$ represents the volume average of a given quantity, i.e. $\langle a\rangle = \frac{1}{|\Omega|}\int_\Omega a\,\mathrm{d}\Omega$. For a detailed derivation of Eq. (18) the reader is referred to [33, 47]. Once the nodal temperatures $\boldsymbol{\theta}_d^*$ are known from the solution of Eq. (18), the solution proceeds by calculating the volume average of the local heat flux as

$$\boldsymbol{Q} = \langle \boldsymbol{q}(\mathbf{x})\rangle = -\frac{1}{|\Omega|}\int_\Omega \boldsymbol{\chi}(\mathbf{x})\boldsymbol{h}(\mathbf{x})\,\mathrm{d}\Omega, \tag{19}$$

to get the macroscopic constitutive law in the form

$$\boldsymbol{Q} = -\boldsymbol{\chi}^{hom}\boldsymbol{H}, \tag{20}$$

where $\boldsymbol{\chi}^{hom}$ stands for the searched homogenized effective conductivity matrix. Note that the components of this matrix follow directly from the solution of two successive steady state heat conduction problems. To

that end, the periodic unit cell is loaded, in turn, by each of the two components of $\boldsymbol{H}$, while the other vanishes. The volume flux averages, Eq. (19), normalized with respect to $\boldsymbol{H}$ then furnish individual columns of $\boldsymbol{\chi}^{hom}$. The required periodicity conditions (the same temperatures $\boldsymbol{\theta}_d^*$ on opposite sides of the unit cell) are accounted for through multi-point constraints. In our particular case it suffice to assign the same code numbers to respective periodic pairs.

A similar dual framework can be formulated for the effective resistivity matrix. Details are available in [47].

In order to compare theoretical predictions with experimental measurements it was necessary to derive the macroscopic estimates of thermal conductivities by repeating the above procedure for the actual laminate. However, instead of discretizing the real meso-structure, the laminate was built from individual homogeneous blocks having the properties derived from the previous homogenization step. The same stacking sequence as evident from Fig. 8 was considered.

Tab. 2: Effective macroscopic thermal conductivities of the laminate $[\mathrm{Wm}^{-1}\mathrm{K}^{-1}]$ (The number in parentheses indicates the difference between a numerical value and experimental data.)

| Analysis | $k$-longitudinal | $k$-transverse |
|---|---|---|
| Prediction | 8.47 (15.3%) | 1.66 (3.75%) |
| Measurement | 10.00 | 1.60 |

Taking into account the possible errors in the determination of phase material parameters (carbon fibers and carbon matrix) on the one hand and errors associated with the laboratory measurements on the other hand, the results summarized in Table 2 are rather encouraging supporting not only the assumed uncoupled three-level homogenization procedure but also the selected computational model reflecting all essential details of the meso-structure including porosity.

# 6 Conclusions and discussion

Several approaches allowing us to treat various types of uncertainties present in actual plain weave carbon-carbon textile composites were reviewed. It is shown that predictions of overall composite response are available either in the context of so called statistically equivalent period unit cell or through applications of micromechanical models depending on the type of supplied microstructural information.

While three-dimensional estimates of overall elastic stiffnesses are available for geometrically imperfect microstructures regardless of the method used, the influence of porosity on the overall behavior has been examined only in the two-dimensional format. Although it is encouraging to see that both the Mori-Tanaka method and FEM simulations performed on the SEPUC deliver comparable results, the fact that both approaches rely on rather different quality of microstructural information somewhat degrades the importance of geometrical imperfections and promotes porosity as a key factor in achieving reliable predictions of the overall response. Incorporating porosity in three-dimensional calculations is therefore highly desirable.

In connection to SEPUC based analyses the credibility of predictions can be extended by introducing three-dimensional data obtained from computer tomography [34]. More tedious approach takes advantage of previously mentioned image analyzer **LUCIA G**. Here, the complex geometry of distinct types of voids is examined by scanning the specimen surfaces during gradual grinding of the specimen cross-section. Simplified geometries of actual voids would, however, be necessary to enable feasible numerical treatment particularly when preparing three-dimensional "periodic" finite element meshes.

Even more restrictive idealization with respect to actual pore geometry is expected with applications of the Mori-Tanaka method. On the microscale (the level of yarns) it appears reasonable to adopt two-dimensional solutions for irregular shaped voids presented in [18, 50]. On the mesoscopic level, however, a family of equivalent ellipsoids will need to be introduced. Moreover, to ensure overall symmetry of the Mori-Tanaka predictions the homogenization procedure will be developed in

a certain hierarchical manner as discussed, e.g. in [50, 39, 47]. A typical sequence would lead to the solution of an auxiliary problem, in which a solitary ellipsoidal inclusion is embedded into an unbounded matrix with the properties found for a geometrically imperfect non-porous composite. For plain weave textile composites the material symmetry of the equivalent homogeneous matrix would be at least orthotropic. While closed form solutions for material systems with transversely-isotropic matrix can be found in [42], no such solutions are available for an orthotropic matrix with the principal material axes different from the axes of the ellipsoid. A numerical evaluation of the Eshelby tensor will therefore be required. For a generally anisotropic matrix this problem was discussed, e.g. in [13].

Resolution of the problems outlined in the last two paragraphs still requires further work. Some of the topics are under current investigation within the scope of the CEZ MSM 6840770003 research project.

## Acknowledgments

The financial support provided by the GAČR grant No. 106/07/1244 and partially also by the research project CEZ MSM 6840770003 is gratefully acknowledged.

## Reference

[1] Y. Benveniste, *A new approach to the application of Mori-Tanaka theory in composite materials*, Mechanics of Materials **6** (1987), 147–157.

[2] Y. Benveniste, G.J. Dvorak, and T. Chen, *On diagonal and elastic symmetry of the approximate effective stiffness tensor of heterogeneous media*, Journal of the Mechanics and Physics of Solids **39** (1991), no. 7, 927–946.

[3] ———, *On effective properties of composites with coated cylindrically orthotropic fibers*, Mechanics of materials **12** (1991), 289–297.

[4] Z. Bittnar and Šejnoha J., *Numerical methods in structural engineering*, ASCE Press, 1996.

[5] T.W. Chow and F.K. Ko, *Textile structural composites*, Elsevier, Amsterdam, 1989.

[6] P.W. Chung and K.K. Tamma, *Woven fabric composites - Developments in engineering bounds, homogenization and applications*, International Journal for Numerical Methods in Engineering **45** (1999), no. 12, 1757–1790.

[7] B.N. Cox and G. Flanagan, *Handbook of analytical methods for textile composites*, Tech. report, NASA Contractor Report 4750, Langley Research Center, 1997, http://hdl.handle.net/2002/15043.

[8] J.D. Eshelby, *The determination of the elastic field of an ellipsoidal inclusion and related problems*, Proceeding of Royal Society, Series A **241** (1957), 376–396.

[9] J. Fish and K. Shek, *Multiscale analysis of large-scale nonlinear structures and materials*, International Journal for Computational Civil and Structural Engineering **1** (2000), no. 1, 79–90.

[10] J. Fish, K. Shek, M. Pandheeradi, and M.S. Shephard, *Computational plasticity for composite structures based on mathematical homogenization: Theory and practice*, Computer Methods in Applied Mechanics and Engineering **148** (1997), 53–73.

[11] J. Fish, Q. Yu, and K. Shek, *Computational damage mechanics for composite materials based on mathematical homogenization*, International Journal for Numerical Methods in Engineering **45** (1999), no. 11, 1657–1679.

[12] Matteo Frigo and Steven G. Johnson, *The design and implementation of FFTW3*, Proceedings of the IEEE **93** (2005), no. 2, 216–231, special issue on "Program Generation, Optimization, and Platform Adaptation".

[13] A.C. Gavazzi and D.C. Lagoudas, *On the numerical evaluation of Eshelby's tensor and its application to elastoplastic fibrous composites*, Computational Mechanics **7** (1990), no. 1, 13–19.

[14] B. Gommers, I. Verpoest, and P. Van Houtte, *The Mori-Tanaka method applied to textile composite materials*, Acta Materialia **46** (1998), no. 6, 2223–2235.

[15] O. Hrstka and A. Kučerová, *Improvements of real coded genetic algorithms based on differential operators preventing the premature convergence*, Advances in Engineering Software **35** (2004), no. 3–4, 237–246.

[16] O. Hrstka, A. Kučerová, M. Lepš, and J. Zeman, *A competitive comparison of different types of evolutionary algorithms*, Computers & Structures **81** (2003), no. 18–19, 1979–1990.

[17] M. Kachanov, *Effective elastic properties of cracked solids: Critical review of some basic concepts*, Applied Mechanics Review **45** (1992), no. 8, 304–335.

[18] M. Kachanov, I. Tsukrov, and B. Shafiro, *Effective moduli of solides with cavities of various shapes*, Applied Mechanics Review **45** (1994), no. 1, 151–174.

[19] M. Košek and B. Košková, *Analysis of yarn wavy path periodicity of textile composites using Discrete Fourier Transform*, Proceeding of International Conference on Composite Engineering ICCE/6 (Orlando, Florida), 1999, pp. 427–429.

[20] M. Košek and P. Seják, *Efficient automated approximation of real yarn waviness in woven composites*, Proceedings of STRUTEX 11 (Liberec, Czech Republic), 2004, pp. 117–124.

[21] B. Košková and S. Vopička, *Determination of yarn waviness parameters for C/C woven composites*, Proceedings of International Conference CARBON '01, Lexington (KY,USA), 2001, pp. 1–6.

[22] ———, *Geometrical aspects of woven composite structure*, Proceedings of International Conference "Reinforced Plastics", Karlovy Vary, Czech Republic, 2001, pp. 96–102.

[23] J. L. Kuhn and P. G. Charalambides, *Elastic response of porous matrix plain weave fabric composites: Part I-Modeling*, Journal of Composite Materials **32** (1998), no. 16, 1426–1471.

[24] ———, *Elastic response of porous matrix plain weave fabric composites: Part II-Results*, Journal of Composite Materials **32** (1998), no. 16, 1472–1507.

[25] ———, *Modeling of plain weave fabric composite geometry*, Journal of Composite Materials **33** (1999), no. 3, 188–220.

[26] A. Kučerová, M. Lepš, and J. Skoček, *Large black-box functions optimization using radial basis function networks*, Proceedings of the Eight International Conference on the Application of AI to Civil, Structural and Environmental Engineering (B.H.V. Topping, ed.), Civil-Comp Press, 2005, on CD ROM.

[27] S.V. Lomov, I. Verpoest, T. Peeters, D. Roose, and M. Zako, *Nesting in textile laminates: Geometrical modelling of the laminate*, Composites Science and Technology **63** (2003), no. 7, 993–1007.

[28] B. Lu and S. Torquato, *Lineal-path function for random heterogeneous materials*, Physical Review E **45** (1992), no. 2, 922–929.

[29] K. Matouš, H.M. Inglis, X. Gua, D. Rypl, and T.L. Jackson, *Multiscale modeling of solid propellants: From particle packing to failure*, Composites Science and Technology **67** (2007), no. 7–8, 1694–1708.

[30] K. Matouš, M. Lepš, J. Zeman, and M. Šejnoha, *Applying genetic algorithms to selected topics commonly encountered in engineering practice*, Computer Methods in Applied Mechanics and Engineering **190** (2000), no. 13–14, 1629–1650.

[31] J. C. Michel, H. Moulinec, and P. Suquet, *Effective properties of composite materials with periodic microstructure: A computational approach*, Computer Methods in Applied Mechanics and Engineering **172** (1999), 109–143.

[32] T. Mori and K. Tanaka, *Average stress in matrix and average elastic energy of elastic materials with misfitting inclusions*, Acta Metallurgica **21** (1973), 571.

[33] I. Özdemir, W. A. M. Brekelmans, and M. G. D. Geers, *Computational homogenization for heat conduction in heterogeneous solids*, International Journal for Numerical Methods in Engineering **0** (2007), 0–0, Article in press.

[34] D. H. Pahr and P. K. Zysset, *FEM surface and volume mesh extraction from CT bone data using a new segmentation method and deformable GVF models*, IEEE Transactions on Medical Imaging **0** (2006), 0–0, Submitted.

[35] M. Palán, *Thermal properties of C-C composites reinforced by textile fabric*, Ph.D. thesis, TU Liberec, 2002, in Czech.

[36] C.M. Pastore, *Quantification of processing artifacts in textile composites*, Composites Manufacturing **4** (1993), no. 4, 217–226.

[37] V. Pešáková, K. Smetana, K. Balík, J. Hruška, M. Petrtýl, H. Hulejová, and M. Adam, *Biological and biochemical properties of the*

*carbon composite and polyethylene implant materials*, Journal of Material Science: Materials in Medicine **14** (2003), 531–537.

[38] R. Piat, I. Tsukrov, N. Mladenov, M. Guellali, R. Ermel, E. Beck, and M.J. Hoffman, *Material modeling of the CVI-infiltrated carbon felt II. Statistical study of the microstructure, numerical analysis and experimental validation*, Composite science and technology **66** (2007), no. 15, 2769–2775.

[39] R. Piat, I. Tsukrov, N. Mladenov, M. Verijenko, M. Guellali, E. Schnack, and M.J. Hoffman, *Material modeling of the CVI-infiltrated carbon felt I. Basic formulae, theory and numerical experiments*, Composite Science and Technology **66** (2007), no. 15, 2997–3003.

[40] D. Rypl, *Sequential and parallel generation of unstructured 3D meshes*, CTU Reports, vol. 2, CTU in Prague, 1998.

[41] J. Schjødt Thomsen and R. Pyrz, *The Mori-Tanaka stiffness tensor: Diagonal symmetry, complex fibre orientations and non-dilute volume fractions*, Mechanics of Materials **33** (2001), 531–544.

[42] I. Sevostianov, N. Yilmaz, V. Kushch, and V. Levin, *Effective elastic properties of matrix composites with transversely-isotropic phases*, International Journal of Solids and Structures **42** (2004), 455–476.

[43] J. Skoček, J. Zeman, and M. Šejnoha, *Effective properties of Carbon-Carbon textile composites: application of the Mori-Tanaka method*, Mechanics of materials **0** (2007), 0–0, Submitted.

[44] B. Tomková, *Study of porous structure of C/C composites*, International Conference ICAPM, Evora, Portugal, 2004, pp. 379–387.

[45] ———, *Modelling of thermophysical properties of woven composites*, Ph.D. thesis, TU Liberec, 2006.

[46] B. Tomková and B. Košková, *The porosity of plain weave C/C composite as an input parameter for evaluation of material properties*, International Conference Carbon 2004, Providence, USA, 2004, p. 50.

[47] B. Tomková, M. Šejnoha, J. Novák, and J. Zeman, *Evaluation of effective thermal conductivities of porous textile composites*, Composites - Part B: **0** (2007), 0–0, Submitted.

[48] S. Torquato, *Random heterogeneous materials: Microstructure and macroscopic properties*, Springer-Verlag, 2002.

[49] S. Torquato and G. Stell, *Microstructure of two-phase random media.I. The n-point probability functions*, Journal of Chemical Physics **77** (1982), no. 4, 2071–2077.

[50] I. Tsukrov, R. Piat, J. Novak, and E. Schnack, *Micromechanical Modeling of Porous Carbon/Carbon Composites*, Mechanics of Advanced Materials and Structures **12** (2005), 43–54.

[51] S. Vopička, *Popis geometrie vyztužujícího systému v tkaninových kompozitech [Description of geometry of textile composites reinforcing system]*, Ph.D. thesis, Technical University of Liberec, 2004, In Czech.

[52] R. Wentorf, R. Collar, M.S. Shephard, and J. Fish, *Automated modeling for complex woven mesostructures*, Computer Methods in Applied Mechanics and Engineering **172** (1999), no. 1–4, 273–291.

[53] J. Whitcomb and K. Sriregan, *Effect of various approximations on predicted progressive failure in plain weave composites*, Composite Structures **34** (1996), no. 1, 13–20.

[54] J. Whitcomb and X.D. Tang, *Effective moduli of woven composites*, Journal of Composite Materials **35** (2001), no. 23, 2127–2144.

[55] C. L. Y. Yeong and S. Torquato, *Reconstructing random media*, Physical Review E **57** (1998), no. 1, 495–506.

[56] J. Zeman, *Analysis of composite materials with random microstructure*, CTU Reports, vol. 7(5), CTU in Prague, 2003, 177 pp.

[57] J. Zeman and M. Šejnoha, *Numerical evaluation of effective properties of graphite fiber tow impregnated by polymer matrix*, Journal of the Mechanics and Physics of Solids **49** (2001), no. 1, 69–90.

[58] ———, *Homogenization of balanced plain weave composites with imperfect microstructure: Part I – theoretical formulation*, International Journal for Solids and Structures **41** (2004), no. 22-23, 6549–6571.

[59] ———, *From random microstructures to representative volume elements*, Modelling and Simulation in Materials Science and Engineering **15** (2007), no. 4, 325–335.

[60] ———, *Homogenization of balanced plain weave composites with imperfect microstructure: Part II – analysis of real world structures*, International Journal for Solids and Structures **0** (2007), 0–0, Submitted.

## List of papers included in disertation

[D1] K. Matouš, M. Lepš, J. Zeman and M. Šejnoha (2000) *Applying genetic algorithms to selected topics commonly encountered in engineering practice*, Computer Methods in Applied Mechanics and Engineering, **190**(13–14), 1629–1650.

[D2] J. Zeman and M. Šejnoha (2001) *Numerical evaluation of effective properties of graphite fiber tow impregnated by polymer matrix* Journal of the Mechanics and Physics of Solids, **44**(2), 37–76.

[D3] M. Šejnoha and J. Zeman (2002) *Overall viscoelastic response of random fibrous composites with statistically quasi uniform distribution of reinforcements* Computer Methods in Applied Mechanics and Engineering, **191**(44), 5027–5044.

[D4] J. Zeman and M. Šejnoha (2004) *Homogenization of balanced plain weave composites with imperfect microstructure: Part I – Theoretical formulation*, International Journal for Solids and Structures, **41**(22–23), 6549–6571.

[D5] M. Lepš and M. Šejnoha (2003) *New approach to optimization of reinforced concrete beams* Computers and Structures, **81**(18–19), 1957–1966.

[D6] M. Šejnoha, R. Valenta and J. Zeman (2004) *Nonlinear Viscoelastic Analysis of Statistically Homogeneous Random Composites* International Journal for Multiscale Computational Engineering, **2**(4), 645–673.

[D7] J. Gajdošík, J. Zeman and M. Šejnoha (2006) *Qualitative analysis of fiber composite microstructure: Influence of boundary conditions*, Probabilistic Engineering Mechanics, **21**, 317–329.

[D8] J. Zeman and M. Šejnoha (2007) *From random microstructures to representative volume elements*, Modelling and Simulation in Materials Science and Engineering, **15**(4), 325–335.

[D9] J. Skoček, J. Zeman and M. Šejnoha (2007) *Effective properties of Carbon-Carbon textile composites: application of the Mori-Tanaka method*, Mechanics of materials, **0**, 0–0, Submitted.

[D10] B. Tomková, M. Šejnoha, J. Novák, and J. Zeman (2007) *Evaluation of Effective Thermal Conductivities of Porous Textile Composites*, Composites - Part B: Engineering, **0**, 0–0, Submitted.

[D11] M. Šejnoha and J. Zeman (2007) *Micromechanical modeling of imperfect textile composites*, International Journal of Engineering Science, **0**, 0–0, Submitted.

[D12] J. Šejnoha, M. Šejnoha, J. Zeman, J. Sýkora and J. Vorel (2007) *A mesoscopic study on historic masonry*, Structural Engineering and Mechanics, **0**, 0–0, Submitted.

[D13] J. Sýkora, J. Vorel, M. Šejnoha and J. Šejnoha (2007) *Analysis of coupled heat and moisture transfer in masonry structures*, Materials and Structures, **0**, 0–0, Submitted.

[D14] J. Novák, J. Zeman, M. Šejnoha, and J. Šejnoha (2007) *Pragmatic multi-scale and multi-physics analysis of Charles Bridge in Prague*, Engineering Structures, **0**, 0–0, Submitted.